

PAPER

Development of GLCM Method in Calculate Entropy Value for Digital Visualization in Identifying Childhood Pneumonia Based on Chest X-Ray Images

Eva Rianti¹(✉), Iskandar Fitri², Sumijan², Finny Fitry Yani^{3,4}

¹Information System, Universitas Putra Indonesia YPTK, Padang, Indonesia

²Information Technology, Universitas Putra Indonesia YPTK, Padang, Indonesia

³Department of Child Health, Faculty of Medicine, Universitas Andalas, Padang, Indonesia

⁴Department of Pediatric, Dr. M. Djamil General Hospital, Padang, Indonesia

evarianti@upiptyk.ac.id

ABSTRACT

Pneumonia can affect people of all ages, especially children. One way to identify pneumonia is by using medical equipment through radiological examinations such as chest X-rays. This study proposes the development of an entropy formula found in the gray level co-occurrence matrix (GLCM) texture extraction method to automatically detect pediatric chest X-ray results in identifying pneumonia. The pre-processing stage is tested with several steps, including converting RGB to grayscale, adaptive histogram equalization (AHE), filtering, Otsu thresholding, image inversion, and automatic image cropping. After preprocessing is the segmentation stage that conducted by processing the image from the cropping results. The testing process in the segmentation stage includes contrast enhancement, Otsu multi-thresholding, border clearing, and image segmentation. The results from the segmentation process are then followed by the extraction stage. The extraction stage focuses on developing the entropy value found in GLCM, referred to as the entropy value algorithm with gray level co-occurrence matrix (EVA-GLCM). The key contributions of this study lie in the advancement of digital image processing methods for the accurate identification of childhood pneumonia through improved texture feature extraction. This study compares the developed entropy value with several previous studies. The development of this entropy value is then followed by the classification stage using a support vector machine (SVM). The accuracy achieved in this study was 97.5%, meaning it was able to accurately detect 390 images out of 400 images. This indicates that the entropy value calculation using the EVA-GLCM formula and classification using SVM can provide more accurate output with a higher accuracy rate.

KEYWORDS

X-ray, extraction, gray level co-occurrence matrix (GLCM), support vector machine (SVM), pneumonia

Rianti, E., Fitri, I., Sumijan, Yani, F.F. (2025). Development of GLCM Method in Calculate Entropy Value for Digital Visualization in Identifying Childhood Pneumonia Based on Chest X-Ray Images. *International Journal of Online and Biomedical Engineering (ijOE)*, 21(2), pp. 137–156. <https://doi.org/10.3991/ijoe.v21i02.52909>

Article submitted 2024-10-15. Revision uploaded 2024-12-05. Final acceptance 2024-12-05.

© 2025 by the authors of this article. Published under CC-BY.

1 INTRODUCTION

Pneumonia is an acute respiratory infection that can infect one or both lungs [1]. Pneumonia can be caused by bacteria, viruses, or fungi present in the air [2]. A healthy immune system typically protects the body from infections, but many factors can weaken this protection [3]. One of the factors that weakens the immune system in children is air pollution [4]. Outdoor air pollution poses a threat to children, especially with the increasing level of urbanization in countries with high pneumonia rates [5]. Indoor air pollution contributes to 62% of child deaths from pneumonia related to air pollution [6]. The lung tissue infected with pneumonia is located in the alveoli. When someone has pneumonia, the alveoli are filled with pus and fluid, making it difficult for the person to breathe and limiting oxygen intake. Approximately 7% of the world's population contracts pneumonia each year, and four million affected patients face a fatal risk.

Information technology in the healthcare field has many advantages, particularly in the processing of digital images taken from various medical imaging tools such as X-rays [7], [8], CT scans [9], [10], and MRIs [11], [12]. These technological advancements offer promising performance in medical image analysis during radiological examinations. One of the most widely used radiological examinations is the X-ray. X-rays are generally performed to view images of the heart, lungs, respiratory tract, blood vessels, and lymph nodes. Chest X-rays of the lungs are used to detect infections in the lungs. One such infection is pneumonia.

Early detection and treatment of pneumonia can reduce child mortality rates [13]. Diagnosing childhood pneumonia is challenging due to the low sensitivity of microbiological tests and weak clinical findings [14]. One of the most important and commonly used techniques for diagnosing childhood pneumonia is chest X-ray imaging [15]. Chest X-rays are a simple, easy, and effective way for doctors to analyze internal organs. However, chest X-rays are difficult to interpret without a radiology expert [16]. Current computational tools still focus on evaluating adult pneumonia, making it difficult to assess pneumonia in children, especially infants. Various methods have been used to evaluate chest X-ray results to achieve accuracy in diagnosing childhood pneumonia, but the routine use of chest radiography for diagnosing childhood pneumonia in outpatient settings is not recommended.

Research conducted [17] discussed a machine learning approach to chest X-rays for detecting pediatric pneumonia. The approach proposed in this research requires data augmentation to balance the classes of the dataset used, optimize the feature extraction scheme, and evaluate the performance of several machine learning models. Image pre-processing and data augmentation were applied by resizing all chest X-ray images to a uniform size and converting them to grayscale. The next stage used AlexNet for this purpose, as it demonstrated a strong ability to provide high pneumonia classification. This study was limited to binary classification of pneumonia using pediatric X-rays with specific resolution and an adequate number of samples.

In 2023, [18] proposed several techniques in their research to analyze chest X-ray images to detect and differentiate between pneumonia and tuberculosis (TB). The techniques used in this research included texture feature extraction using gray level co-occurrence matrices (GLCM), VGG16, ResNet18, and SVM. The results obtained an accuracy rate of 99.6%, sensitivity of 99.17%, specificity of 99.42%, precision of 99.63%, and an AUC of 99.58% in distinguishing between pneumonia and TB. Further research was conducted [19]. This study proposed pneumonia detection divided into two stages: mild pneumonia and severe pneumonia. The stages involved feature extraction for both mild and severe pneumonia using several methods such

as CLAHE, SVM, GLCM, and random forest. The accuracy rate and parameters using random forest yielded better results than other models, reaching 83.11%.

The key contributions of this study lie in the advancement of digital image processing methods for the accurate identification of childhood pneumonia through improved texture feature extraction. Specifically, this study builds upon the foundational research [19] and [20], focusing on refining the GLCM algorithm to enhance texture analysis capabilities. Unlike previous studies that primarily applied standard texture extraction or machine learning models, this study proposes a novel development of the GLCM algorithm to achieve more precise and discriminative texture features from chest X-ray images. The enhancement of GLCM aims to address the challenges of low sensitivity and limited specificity found in existing computational tools, thereby offering a method that improves the robustness and accuracy of pneumonia diagnosis in children. By optimizing the GLCM model for texture extraction, this research contributes a significant step toward creating reliable and effective diagnostic support tools, which are crucial for medical practitioners, particularly in settings with limited access to specialized radiology expertise. The outcomes are expected to lead to a higher accuracy rate in detecting childhood pneumonia and to facilitate earlier and more reliable diagnoses, ultimately aiding in the reduction of pediatric mortality rates linked to respiratory infections.

2 MATERIALS AND METHODS

2.1 Research framework

This study was conducted with the aim of improving the quality of X-ray images in identifying childhood pneumonia by developing a texture extraction method using the GLCM algorithm. The research framework can be seen in Figure 1 below:

In this study, the initial step was the collection of chest X-ray images of children. These images were then categorized based on their type, specifically identifying which X-rays indicated pneumonia or other lung diseases. The X-ray images of children diagnosed with pneumonia were selected and processed in the following steps, while images of other lung diseases were set aside. The next stage was pre-processing, which in this study included the following steps: converting RGB to grayscale, adaptive histogram equalization (AHE), object filtering, and Otsu thresholding. The following stage was segmentation, which in this research involved contrast enhancement, Otsu multi-thresholding, clearing borders, and image segmentation. The next step was feature extraction, where the focus was on developing the GLCM method, particularly in the search for entropy values. The final stage was classification, where the images were grouped into three categories: severe pneumonia, mild pneumonia, and normal, using the SVM method. Below is an explanation of each research stage:

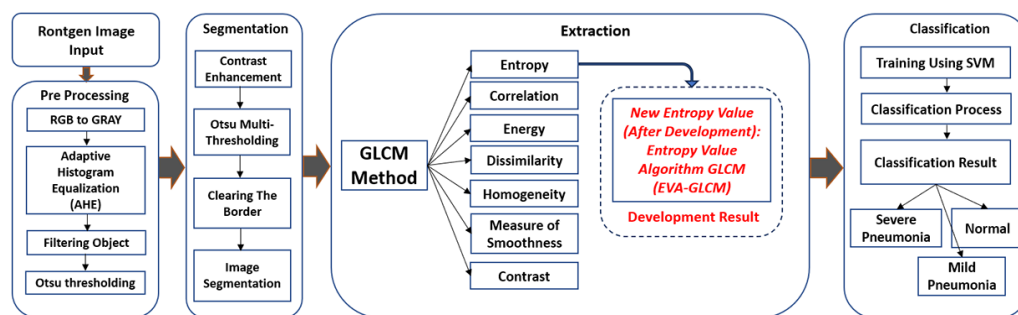


Fig. 1. Research framework

2.2 Research framework details

Data collection and grouping. The collection of X-ray images was taken from the SIEMENS MULTI SELECT DR X-ray machine owned by the Radiology Department of the Regional General Hospital (RSUD) Dr. Rasidin in Padang City. The images collected were chest X-rays of children's lungs. This research tested a total of 400 pediatric chest X-ray images. The test data in the form of chest X-rays consisted of three types of health conditions in children's lungs, namely 170 severe pneumonia, 130 mild pneumonia, and 100 normal. The X-ray images were obtained from the Radiology Department, specifically children's chest X-rays, and also from a public dataset from the internet. The data was categorized into images identified as pneumonia and other lung diseases.

Pre-processing. Pre-processing involves image acquisition as input, obtaining grayscale images, noise filtering, and creating binary images. Preprocessing is also an advanced process used to normalize images without losing color, texture, intensity, or information. This research includes several preprocessing steps, explained below.

1. Chest X-ray image input. The image input process is done using pediatric chest X-ray images. Image input is performed after the data is categorized based on pediatric chest X-ray images identified with pneumonia or other lung infections.
2. RGB to grayscale. The initial step in preprocessing is converting the original image, which is in RGB format, to grayscale. This aims to change the original image's color so that the pixel intensity is represented in shades of gray.
3. Adaptive histogram equalization (AHE). AHE is a technique used in digital image processing to enhance the contrast of an image by adjusting the pixel intensity values. AHE is especially useful in medical image processing because it enhances image contrast and clarifies details, particularly in images with complex contrast variations.
4. Filtering. The goal of the filtering stage is to modify the appearance of the image by altering pixel colors, enhancing contrast, adding special effects, and removing noise around the characters in the image.
5. Otsu thresholding. Otsu thresholding is an image processing method based on the intensity histogram of the image [21]. Its purpose is to find the threshold value by separating the histogram into two groups, thereby minimizing the inter-class variance between the two groups [22].

Segmentation. Segmentation is the process of dividing an image into several smaller parts [23]. The main goal of image segmentation is to identify object boundaries or contours, separate objects from the background, and group image pixels into different clusters based on certain characteristics such as color, intensity, texture, or shape [24]. In this research, several steps were taken to achieve the desired segmentation result for the object. The steps taken to achieve the appropriate segmentation result for the research object are contrast enhancement, Otsu multi-thresholding, and clearing the border.

1. Contrast enhancement. Contrast enhancement is a technique in image processing aimed at increasing the difference between bright and dark areas in an image, making features that may not be visible in the original image easier to recognize.
2. Otsu Multi-Thresholding. This step is performed to achieve image segmentation with more than two threshold levels. The process aims to automatically calculate the optimal threshold and separate the object from the background in a binary

image (with two threshold levels). In this research, the image contains more than two groups of pixels and will be classified into several classes based on intensity or certain features.

3. Clearing the border. This step aims to remove or replace pixel values around the image border with specific values, making it easier to isolate or process objects within the image. This process is often used to eliminate effects caused by artifacts around the image edges, which can interfere with further analysis or processing.
4. Image segmentation. The segmentation process is carried out after the clearing the border step, with the goal of dividing the image into different parts based on specific characteristics. The characteristic used for segmentation in this process is the texture of the pediatric lung X-ray image.

Texture feature extraction: GLCM method. Image extraction is the process of extracting important information or features from a digital image for analysis and further processing. The purpose of image extraction is to reduce the dimensionality of image data and capture relevant information from the image. The type of image extraction used in this research is texture feature extraction. Texture feature extraction is a process that describes the textural properties of an image. The goal of texture features is to identify patterns, structures, or texture characteristics within an image. In this research, the texture extraction method used is GLCM [25]. The steps in the GLCM process involve calculating the frequency of pixel intensity pairs occurring at a specific distance and direction. In this study, GLCM can extract features such as entropy, contrast, correlation, energy, homogeneity, dissimilarity, and measure of smoothness [26]. The study focused on developing the GLCM algorithm, particularly in calculating the entropy value. Entropy is one method used to measure image complexity by considering neighboring pixels and providing insight into the complexity and uncertainty of the pixel intensity distribution within the image. This method involves calculating the entropy of each pixel by taking into account the values and distribution of neighboring pixels in a certain region. By calculating entropy, we can analyze and process images for various purposes such as segmentation, compression, and pattern recognition, which can help improve the quality and efficiency of digital image processing applications.

1. Entropy before development: The steps performed on entropy before this development involved calculating the entropy value using the basic entropy formula and the modified entropy formula from previous researchers. The first formula, which is basic entropy, is obtained from the book Computer Vision and Image Processing Fundamentals and Applications, with the following formula [27]:

$$Entropy = -\sum_i \sum_j p[i, j] \log_p [i, j] \quad (1)$$

Where: \sum_i = sum of all elements in row (i) of the probability distribution, \sum_j = sum of all elements in column (j) of the probability distribution, $P[i, j]$ = the joint probability of elements (i, j) in the two-dimensional probability distribution, $\log_p [i, j]$ = the logarithm of the joint probability ($p[i, j]$).

The basic entropy formula in the above equation is used to calculate the probability of pixel pairs with intensities i and j in GLCM using a base-2 logarithm [28]. The entropy value calculation using the basic formula before development is done by calculating the pixel pairs in each row and column, starting from row = 1 and column = 1.

The basic entropy formula that existed previously, as explained above, was developed by another researcher [29]. This researcher made modifications to the initial and final iteration values of the summation, where in this case it started from $i = 2$ to $i = 2v_g$, resulting in the formula contained in the equation below:

$$Entropy = \sum_{i=2}^{2v_g} \log(F(i, j) \times F(i, j)) \tag{2}$$

Where: $(i = 2) (2v_g)$ = Addition operation from i (row) = 2 to $i = 2v_g$ by adding the elements in this range, $\log F(i, j)$ = Logarithm operation applied from joint probability, $F(i, j)$ = probability of element (i, j) .

- Entropy after development: The entropy formula that has been developed by previous researchers was Contribution (development result) is obtained by developing the basic entropy formula redeveloped in this study to produce a new one to obtain a better entropy result. The derivation of the entropy formula is carried out based on the previous formula contained in equation 3, which meets the following conditions:

$$\sum_{i=2}^{2v_g} (\log f(i, j)) f(i, j) > \frac{\sum_i^x (\log f(i, j)) f(i, j)}{4}$$

$$\frac{\sum_i^x (\log f(i, j)) f(i, j)}{4} \geq \frac{\sum_i^x (\log f(i, j)) f(i, j) + \sum_k^x (\log f(k, l)) f(k, l) + \sum_m^x (\log f(m, n)) f(m, n) + \sum_o^x (\log f(o, p)) f(o, p)}{4}$$

At this stage, entropy is calculated in 4 directions, namely $\theta = 0^\circ, 45^\circ, 90^\circ, 135^\circ$

$$\frac{\sum_i^x (\log f(i, j)) f(i, j)}{4} \geq \left(\frac{\sum_i^x \sum_j^y (\log f(i, j)) f(i, j) + \sum_k^x \sum_l^y (\log f(k, l)) f(k, l)}{4} + \frac{\sum_m^x \sum_n^y (\log f(m, n)) f(m, n) + \sum_o^x \sum_p^y (\log f(o, p)) f(o, p)}{4} \right) \tag{3}$$

$$\frac{\sum_i^x (\log f(i, j)) f(i, j)}{4} \geq \frac{\sum_i^x \sum_j^y (\log f(i, j)) f(i, j)}{4} + \frac{\sum_k^x \sum_l^y (\log f(k, l)) f(k, l)}{4} + \frac{\sum_m^x \sum_n^y (\log f(m, n)) f(m, n)}{4} + \frac{\sum_o^x \sum_p^y (\log f(o, p)) f(o, p)}{4}$$

The equation above can be seen that, on the right side, there is an entropy calculation for 4 directions; if averaged, the value will be smaller or the same as the left side. A more complete explanation of the calculation is as follows: For example, rows and columns in the co-occurrence matrix with directions, for, for, and for, then (2) is the entropy value for each matrix by adding columns so that (1) (2) or

$$\sum_i^{2Vg} (\log f(i, j))f(i, j) \geq \frac{\sum_i^x (\log f(i, j))f(i, j)}{4} \geq \frac{\sum_i^x \sum_j^y (\log f(i, j))f(i, j)}{4} + \frac{\sum_k^x \sum_l^y (\log f(k, l))f(k, l)}{4} + \frac{\sum_m^x \sum_n^y (\log f(m, n))f(m, n)}{4} + \frac{\sum_o^x \sum_p^y (\log f(o, p))f(o, p)}{4} \tag{4}$$

If we assume that each entropy is E , then equation (2) can be written more simply as in the equation below.

$$\Rightarrow \sum_i^{2Vg} (\log f(i, j))f(i, j) \geq \frac{\sum_i^x (\log f(i, j))f(i, j)}{4} \geq \frac{E_{0+} E_{45+} E_{90+} E_{135}}{4}$$

Average entropy can be defined as total entropy E_t that is

$$E_t = \frac{\sum_i^x \sum_j^y (\log f(i, j))f(i, j)}{4} + \frac{\sum_k^x \sum_l^y (\log f(k, l))f(k, l)}{4} + \frac{\sum_m^x \sum_n^y (\log f(m, n))f(m, n)}{4} + \frac{\sum_o^x \sum_p^y (\log f(o, p))f(o, p)}{4} = \frac{E_{0+} E_{45+} E_{90+} E_{135}}{4} \tag{5}$$

The above description shows that the basic entropy has a greater value than the total entropy developed through current research. Where: $\sum_i, \sum_k, \sum_m, \sum_o$ = Sum of pixel values for each row i, k, m, o , $\sum_j, \sum_l, \sum_n, \sum_p$ = Sum of pixel values for each row j, l, n, p , $f(i, j), f(k, l), f(m, n), f(o, p)$ = Probability of pixel values in rows and columns, $(i, j), (k, l), (m, n), (o, p)$, $\log(f(i, j)), \log(f(k, l)), \log(f(m, n)), \log(f(o, p))$ = base 2 logarithm value of the probability of pixel values in rows and columns $(i, j), (k, l), (m, n), (o, p)$.

The entropy formula developed in this research is presented in equation 5, where the equation is derived from the formula in equation 1. The image objects used in this research are children’s lung X-ray images. For good results, the entropy value obtained should be low, not high, because high entropy causes noise to be visible. The higher the entropy value, the more complex and random the texture in the image. High entropy can make the image appear more blurred or difficult to interpret by doctors or medical professionals. Low entropy in an X-ray image indicates that the image has a more stable intensity. This allows the important structural details needed to detect childhood pneumonia to be more clearly visible in the lung area. The development of the entropy formula carried out in this study can provide lower entropy values compared to the two previous entropy formulas because the formula developed in this study is capable of providing a more accurate and comprehensive measure of texture diversity in the image by considering the direction of different pixel pairs. This is part of the research’s contribution (development result), called the extended visual assessment with gray level co-occurrence matrix (EVA-GLCM).

Classification. Classification is the process of grouping images into specific categories based on certain characteristics [30]. The classification process in this research was conducted based on the results of processing children’s lung X-ray data to identify lungs infected with mild pneumonia, severe pneumonia, and normal lungs. The data processed in this research consists of 400 images. The processed data in

the form of chest X-rays consisted of three types of health conditions in children’s lungs, namely 170 severe pneumonia, 130 mild pneumonia, and 100 normal. The classification stages in this research used the SVM. SVM is an algorithm in machine learning used for classification and regression tasks. SVM seeks the optimal separator between two data classes in the feature space.

Accuracy. Accuracy is a method used to measure how well the results of image processing or analysis reflect reality or meet the desired objectives [31]. Accuracy is crucial in various applications such as image segmentation, pattern recognition, edge detection, and object classification. High accuracy indicates that the model or algorithm can be trusted for specific image processing tasks [32]. This study used 400 images to group data from X-ray images of mild pneumonia, severe pneumonia, and normal lungs. The accuracy achieved in this study was 97.5%, meaning it was able to accurately detect 390 images out of 400 images with the following distribution: correctly detect 167 images out of 170 severe pneumonia with three inaccurate images, correctly detect 126 images out of 130 mild pneumonias with four inaccurate images, and correctly detect 97 images out of 100 normal with three inaccurate images.

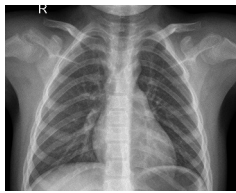


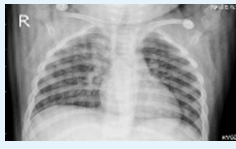


3 RESULTS

The data tested in this research consists of 400 children’s lung X-ray images, which were then processed through several stages to achieve results in line with this research. These stages include preprocessing results, segmentation results, texture extraction results using the GLCM matrix, which focuses on entropy development to measure diversity or complexity in the children’s lung X-ray images, and classification using support vector machine.

3.1 Input image

The number of data tested is 400 images. The data in the form of chest X-rays consisted of three types of health conditions in children’s lungs, namely 170 severe pneumonia, 130 mild pneumonia, and 100 normal. These data will be tested through several stages, namely pre-processing, segmentation, extraction, and classification, to obtain information on the detection of mild pneumonia, severe pneumonia, and normal. As a sample in this paper, we present six test images with details of two images of severe pneumonia, two images of mild pneumonia, and two images of normal. The chest X-ray images of children used in this study as initial data and input data can be seen in Table 1.

Table 1. Input image

No	Severe Pneumonia	No	Mild Pneumonia	No	Normal
1		3		5	
2		4		6	

3.2 Pre-processing






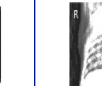







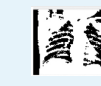












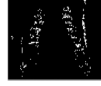




















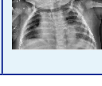
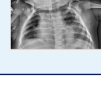





The first preprocessing stage is converting the original X-ray image into a grayscale image. This is done to clearly distinguish between the lung area and the non-lung area of the image. The second preprocessing stage is AHE, aimed at improving image quality. The third preprocessing stage is filtering, which involves removing noise from the input image after AHE has been applied. The fourth preprocessing stage involves further testing the image by enhancing the threshold value using Otsu thresholding, a technique designed to segment the image automatically and effectively. The results of the preprocessing stages, including RGB to grayscale conversion, AHE, filtering, and Otsu thresholding, are provided. The results of image testing in the preprocessing stages are shown in Table 2.

3.3 Segmentation

The cropping results from the preprocessing stage are then followed by the segmentation stage. In this segmentation stage, several methods are used, including contrast enhancement, multi-Otsu thresholding, border clearing, and image segmentation. The results of contrast enhancement are then processed in the multi-Otsu thresholding stage. The next stage is border clearing. The results from the border clearing process are then passed on to the next stage, which is image segmentation. This stage will produce an output image that meets the required object detection criteria. The segmentation testing process can be seen in Table 2. The testing was conducted on 20 children's lung images. These 20 images consist of eight images identified with mild pneumonia, six images identified with severe pneumonia, and four normal lung images. As a sample for this research, we displayed six children's lung images, consisting of two images identified with mild pneumonia, two images identified with severe pneumonia, and two normal lung images. The image testing is conducted based on the cropping results and then proceeds to the contrast enhancement stage, which aims to clarify the visual differences between various elements in the image features, making them clearer and easier to see. The images processed with contrast enhancement are then passed to the next stage, which is multi-Otsu thresholding. The use of the multi-Otsu thresholding technique aims to find threshold values at more than two levels to obtain the optimal threshold value from the pixels, as this research involves grouping the images into two classes based on the intensity values of each feature.

The image processed using multi-Otsu thresholding is then followed by the border-clearing stage, using the clearing the border technique to improve segmentation accuracy, reduce errors in analysis, enhance visualization, and facilitate object detection and recognition. The final stage of segmentation is displaying the results of the image segmentation. This image segmentation stage is carried out with the aim of separating the image from its background to isolate the desired object and obtain an image with specific characteristics. The result of this image segmentation is then passed on to the texture extraction stage. In this research, the texture extraction stage is conducted by developing the entropy value in GLCM, referred to as the entropy value algorithm – gray level co-occurrence matrix.

Table 2. Input image, pre-processing result image, and segmentation result image

No	Input Image	Preprocessing Result Image				Segmentation Result Image			
		RGB to Grayscale	AHE	Filtering	Otsu Thresholding	Contrast Enhancement	Multi Otsu Thresholding	Clearing the Border	Image Segmentation
1									
2									
3									
4									
5									
6									

3.4 Texture extraction


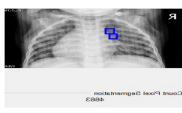
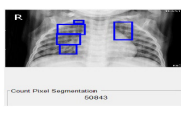

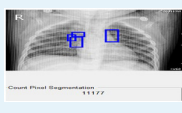
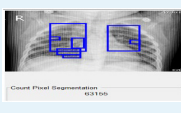
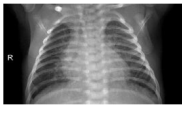
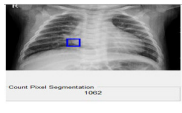
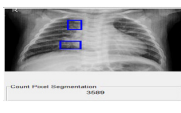

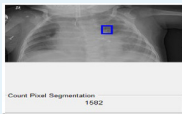







The texture extraction tested in this study uses the processed images obtained in the previous segmentation stage. At the segmentation stage, the object image has already been separated from the background. The results of the segmentation are then processed using the GLCM matrix. Calculations and tests using the GLCM matrix involve measuring the values of entropy, contrast, correlation, energy, homogeneity, dissimilarity, and the measure of smoothness in each test image. The testing was conducted on 20 chest X-ray images of children, consisting of eight images with severe pneumonia, eight images identified with mild pneumonia, and four normal lung images. As a sample for this research, we displayed six children's lung images, consisting of two images identified with mild pneumonia, two images identified with severe pneumonia, and two normal lung images.

The development result of this study focuses on developing the formulation for calculating entropy values in the GLCM method. The results of feature extraction testing and visualization with the basic entropy formula (before development) and the EVA-GLCM entropy formula can be seen in Table 3 below, which compares the two testing results of entropy values and image visualization.

The development result of this study lies in the development of an entropy formula. The development of the entropy formula in this research helps describe the level of uncertainty or complexity of the texture in the images, as the lung X-rays processed in this research have a high level of complexity. With the improvements made to the entropy formula used in this research, it is possible to measure the quality of the image after testing. Images with high entropy values indicate that the image contains a lot of noise, with evenly distributed pixel pairs, less structure, and more blurriness, making interpretation difficult. On the other hand, images with low

entropy values indicate that the image is more stable and makes it easier to detect the desired object.

Table 3. Texture extraction test results with basic entropy formula (before development) and entropy formula development (EVA-GLCM)

No	Input Image	Entropy Before Development (Standard GLCM Method)		Entropy After Development (EVA-GLCM Method)	
		Value	Visualization	Value	Visualization
1		13.26		1.92	
2		14.09		1.9333	
3		13.01		1.99	
4		12.01		1.72	
5		13.36		1.85	
6		13.53		1.81	

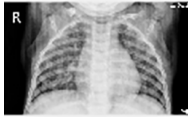
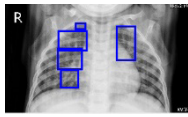

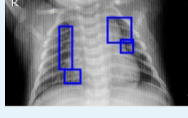

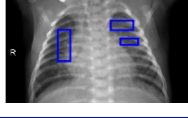

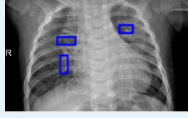




The development of the formula, based on the basic entropy formula, has resulted in a new formula that serves as the development result of this research. The newly developed entropy formula in this research is named the EVA-GLCM. Based on Table 5, it can be proven that the entropy values tested for each image are significantly lower compared to tests using the basic formula. The development result of the entropy formula discovered in this study results in better image quality and makes it easier to identify children’s lung X-rays that are diagnosed with pneumonia compared to the use of the entropy formula from the two previous methods, which consistently produced high entropy values for each test image.

3.5 Classification

The results of the tests, whose values were calculated using the GLCM matrix in the texture extraction, will then be processed to classify the test images into three result groups: images identified as mild pneumonia, severe pneumonia, and normal. The image classification for testing at the classification stage is performed using a SVM. This SVM process is carried out through several testing steps. The first stage in

the SVM process involves training all the input data obtained from children’s chest X-ray images. This data is then tested to achieve data classification. The data classification results from the SVM testing produce three data groups identified from the X-ray results: mild pneumonia, severe pneumonia, and normal. The final stage of this classification process is to obtain the accuracy rate of all the tested data. The accuracy rate obtained from this classification process is 96%. The classification test results can be seen in Table 4.

Table 4. Classification results using SVM

No	Rontgen Image	Object Detection	Pixel Number	Classification
1			Count Pixel Segmentation 50843	Predict Result Pneumonia - Berat
2			Count Pixel Segmentation 63155	Predict Result Pneumonia - Berat
3			Count Pixel Segmentation 18604	Predict Result Pneumonia - Ringan
4			Count Pixel Segmentation 3589	Predict Result Pneumonia - Ringan
5			Count Pixel Segmentation 0	Predict Result Normal
6			Count Pixel Segmentation 0	Predict Result Normal

The comparison of previous research conducted by Saroj Agrawal and Eva Rianti can be seen in Table 5. In Saroj Agrawal’s research, the data processing included a preprocessing stage but only involved one step of noise cleaning in the image, using the CLAHE technique. However, the cropping and segmentation stages were not explained in that research. For the extraction stage, Saroj Agrawal used the GLCM matrix but focused solely on optimizing pixel values for children’s lungs infected with pneumonia. Saroj Agrawal used SVM and random forest for the image classification process and grouped the images into mild and severe pneumonia categories, achieving an accuracy rate of 85%. The accuracy achieved in this study was 97.5%, meaning it was able to accurately detect 390 images out of 400 images with the following distribution: correctly detect 167 images out of 170 severe pneumonia with three inaccurate images, correctly detect 126 images out of 130 mild pneumonias with four inaccurate images, and correctly detect 97 images out of 100 normal with three inaccurate images.

Based on these two previous studies, the author of this research performed several stages on the lung images, including preprocessing to obtain automatic

cropping, focusing on the object to be processed, and continuing to the segmentation stage to remove noise from the object. Saroj Agrawal focused only on calculating the overall pixel values from X-ray results identified as pneumonia. In this research, the author developed the entropy formula in the GLCM, named the EVA-GLCM. The development of this entropy value was carried out to improve image quality by producing much lower entropy values, resulting in a structured pixel pair probability distribution that is easy to analyze, especially for medical images.

4 DISCUSSION

4.1 Input image discussion

Table 1 presents the results of chest X-ray image classification, categorized into three distinct groups: Severe pneumonia, mild pneumonia, and normal. Each image in the table shows specific radiographic patterns, indicating that the classification model used, possibly based on machine learning or deep learning, has successfully differentiated the severity levels of lung infection from the radiographic images. In the severe pneumonia group, images one and two exhibit typical characteristics of severe pneumonia, such as increased opacity, extensive lung consolidation, and significant deviation from normal lung patterns. The visible infiltrates indicate widespread infection, consistent with clinical symptoms of severe pneumonia, where lung function is significantly impaired. The images in the mild pneumonia category (numbers three and four) show more localized and less dense infiltrates compared to the severe pneumonia category. This pattern is consistent with mild pneumonia, where only a small portion of the lungs is affected by the infection. The classification model appears to have successfully distinguished mild pneumonia from severe pneumonia and normal lungs, demonstrating its sensitivity in detecting the early stages of lung infection. For the normal category (numbers five and six), the images show clear lungs without any signs of consolidation or opacity, characteristic of healthy lungs.

4.2 Pre-processing and segmentation discussion

Table 2 provides a detailed overview of the image preprocessing and segmentation pipeline applied to chest X-ray images for the detection and analysis of lung abnormalities. The table is divided into three main sections: 1) Input Image, 2) Pre-processing result image, and 3) Segmentation result image. Each section illustrates the transformation that the images undergo as part of the image processing workflow, which includes multiple steps aimed at enhancing the image for better segmentation and analysis. The results in Table 2 suggest that the preprocessing and segmentation pipeline is highly effective in preparing chest X-ray images for diagnostic analysis. Each step in the preprocessing pipeline contributes to improving the quality of the images and ensuring that the lung structures are accurately segmented. The RGB to grayscale conversion and AHE steps provide a strong foundation by enhancing the contrast and simplifying the images. The Otsu thresholding and multi-Otsu thresholding steps effectively separate the lung regions from the background, which is crucial for subsequent diagnostic tasks. The clearing of borders ensures that artifacts and irrelevant regions do not interfere with the analysis, improving the overall precision of the segmentation. The preprocessing and segmentation workflow presented in Table 2

successfully transforms raw chest X-ray images into well-segmented lung regions, which can then be used for further analysis. This process is critical in medical imaging, where accurate segmentation of lung fields is essential for the detection of diseases such as pneumonia. The workflow's robustness, with multiple noise-reducing and contrast-enhancing steps, ensures that even challenging images, such as those with low contrast or noise, can be processed effectively. This segmentation process can be highly beneficial in the automation of pneumonia detection or other lung conditions, ultimately contributing to improved diagnostic accuracy in clinical settings.

4.3 Texture extraction discussion

Table 3 presents a comparison of texture extraction results using two different entropy-based formulas applied to chest X-ray images. The first method, entropy before development, employs the basic entropy formula to quantify the texture, while the second method, entropy after development, uses an advanced entropy calculation based on the EVA-GLCM technique. The table is organized into three key sections: Input image, entropy Before development (with value and visualization), and entropy after development (with value and visualization). The analysis aims to evaluate how the entropy values and their visual representations differ between the two methods and how they contribute to improved texture extraction in medical image analysis.

The second section of the table showcases the results of the basic entropy formula applied to the input images. Entropy is a statistical measure that quantifies the randomness or complexity of pixel intensities in an image, which is useful for analyzing texture. Entropy values: The values in this column range from 12.08 to 13.53, indicating a moderate level of texture complexity across the six images. Higher entropy values suggest more variability in pixel intensities, which can be indicative of complex textures within the lung fields. Visualization: The visualizations associated with these values show pixel segmentation results. The segmentations, however, appear relatively coarse, with large uniform regions that may not capture all the fine-grained details in the lung texture. This suggests that the basic entropy method might not be fully capable of highlighting intricate structures within the X-rays, leading to less precise diagnostic outcomes.

The third section represents the results of an enhanced entropy formula, leveraging the EVA-GLCM method. This method combines entropy with GLCM to provide a more detailed analysis of texture patterns, capturing both local and global pixel relationships. Entropy values: The entropy values for the developed formula are significantly lower, ranging from 1.81 to 2.03. These lower values reflect a more refined focus on specific texture regions of interest, rather than the broader, less detailed approach of the basic entropy formula. The decreased entropy indicates that the method is better at isolating key features within the X-ray, such as lung structures affected by disease. Visualization: The visualizations in this column demonstrate clear improvements in segmentation. The blue bounding boxes highlight distinct regions of interest within the lung fields, providing a more targeted approach to texture analysis. The improved segmentation is particularly evident in the precise delineation of lung boundaries and pathological areas. These visualizations suggest that the EVA-GLCM method is more effective in isolating relevant texture information, which is crucial for identifying abnormalities in chest X-rays.

The lower entropy values after development suggest that the enhanced formula can focus on more specific, diagnostically relevant texture patterns. By reducing

the overall complexity and isolating key regions, the EVA-GLCM method provides a more detailed analysis of the lung texture. The segmentation results after development are much more precise, with clear identification of areas that likely correspond to pathological features. In contrast, the basic entropy method produces broader, less focused segmentations, which could lead to less accurate diagnoses. The improvement in both entropy values and visual segmentation demonstrates that the EVA-GLCM method provides a more nuanced and effective approach to texture analysis in medical images. This enhanced method can contribute to better diagnostic accuracy by more clearly highlighting abnormalities within the lung fields, which are critical for detecting conditions such as pneumonia.

4.4 Classification discussion

Table 4 presents the classification outcomes of chest X-ray images using a SVM classifier. The table is divided into four key columns: Rontgen image, object detection, pixel number, and classification. This analysis focuses on how the SVM classifier, using pixel segmentation and object detection, successfully identifies the presence of pneumonia and classifies it into different severity levels, such as severe pneumonia, mild pneumonia, and normal cases.

The SVM classifier demonstrates high accuracy in distinguishing between severe pneumonia, mild pneumonia, and normal cases. The use of object detection and pixel segmentation provides a robust methodology for focusing on the relevant lung regions, reducing the likelihood of misclassification. The classifier's performance can be evaluated based on the following criteria: The classifier accurately identifies cases of severe pneumonia by detecting large pathological regions and assigning high pixel counts. This suggests that the SVM model is sensitive to extensive lung abnormalities, which is critical for detecting high-risk cases. The classifier also performs well in detecting mild pneumonia cases, as indicated by the smaller regions of interest and lower pixel counts. This ability to differentiate between mild and severe pneumonia is vital for providing appropriate medical interventions. The classifier successfully identifies normal cases with a pixel count of zero and no detected abnormalities. This high specificity ensures that healthy lungs are not incorrectly classified as diseased, avoiding unnecessary medical treatments.

The results presented in Table 4 highlight the effectiveness of the SVM classifier in analyzing chest X-ray images for the detection and classification of pneumonia. By combining object detection and pixel segmentation, the classifier is able to accurately differentiate between severe pneumonia, mild pneumonia, and normal cases. The pixel count serves as a quantitative measure of the extent of the disease, supporting the classification decisions. These results suggest that the SVM-based system could be a valuable tool in clinical settings for the early detection and classification of pneumonia, ultimately leading to more timely and effective treatments for patients.

4.5 Comparative and accuracy discussion

The current research does not explicitly elaborate on the use of standard performance metrics such as precision, recall, and F1-score. Integrating a discussion on these metrics could provide a clearer comparative analysis of the proposed EVA-GLCM method's performance against traditional and recent algorithms. Precision would highlight the method's ability to correctly identify positive cases, recall would show

its capacity to detect actual positive cases, and the F1 score would offer a balance between the two, ensuring a comprehensive evaluation. Discussing these metrics could strengthen the case for the superiority of EVA-GLCM and SVM over prior techniques. The significance of this research lies in its theoretical and practical contributions. Theoretically, it advances the field of digital image processing by developing the EVA-GLCM algorithm, which offers a more nuanced approach to texture analysis in medical imaging. This development allows for a lower entropy calculation, leading to clearer, more structured images that improve interpretability and diagnostic accuracy. Practically, the implementation of this algorithm can enhance clinical workflows by providing a reliable, automated system for identifying pneumonia in pediatric chest X-rays. This is particularly beneficial in healthcare settings with limited radiology expertise, aiding in quicker, more accurate diagnoses and contributing to reduction in child mortality rates.

Conducting a comparative analysis using metrics such as accuracy, precision, recall, and F1-score would provide a clear determination of which model—EVA-GLCM with SVM or other existing models—is the most efficient for identifying childhood pneumonia. This analysis would highlight strengths and weaknesses and provide a data-driven recommendation for clinical use. Incorporating additional performance metrics such as precision, recall, and F1-score would present a more comprehensive picture of the model's performance. These metrics are crucial in medical diagnostics to evaluate false positives and negatives, ensuring a reliable method that minimizes diagnostic errors. Evaluating the real-world implications of this method involves assessing its integration into clinical settings, considering the computational demands of the EVA-GLCM and SVM classification process. It is essential to determine if standard healthcare hardware can support these computational processes without requiring significant upgrades or adaptations. The authors may consider exploring image enhancement techniques in other domains, such as the wavelet domain, where methods like continuous wavelet transform (CWT) have shown promising results in improving image detail and quality. Integrating such approaches could potentially enhance the current pre-processing and feature extraction pipeline.

5 CONCLUSION

The key contributions of this study lie in the advancement of digital image processing methods for the accurate identification of childhood pneumonia through improved texture feature extraction. The development of the entropy formula in this research involved modifying the previous entropy formula into the EVA-GLCM. The result of this modification was an improvement in image quality, as the entropy value obtained became smaller compared to the previously used entropy formula. The development result of this study has a significant impact on education, particularly in the field of digital image processing. The development of the EVA-GLCM in this study proves that the image quality is better than that produced by the earlier entropy formulas, as it generates a lower entropy value and enhances the image quality. A lower entropy value indicates that the image contains less noise, is more structured, more stable, and facilitates the detection of desired objects, particularly in the analysis of medical images for identifying pneumonia in children using X-ray images. The testing of the developed entropy formula allows conclusions to be drawn. The development of a new formula in texture extraction using GLCM to identify pneumonia in children through X-ray images was successful. The testing of the entropy

formula in the GLCM matrix, through the derivation of the EVA-GLCM, resulted in a lower entropy value compared to the basic entropy formula and those modified by previous researchers, thus producing better image quality. The accuracy achieved in this study was 97.5%, meaning it was able to accurately detect 390 images out of 400 images with the following distribution: correctly detect 167 images out of 170 of severe pneumonia with three inaccurate images, able to correctly detect 126 images out of 130 of mild pneumonia with four inaccurate images, and able to correctly detect 97 images out of 100 of normal with three inaccurate images. The application of pneumonia identification in children using X-ray images in this research can determine the infected area of the lungs by detecting objects in the lung region and displaying the number of pixels in the image. The higher the number of displayed pixels, the larger the lung area identified, and conversely, the lower the number of pixels, the smaller the lung area identified. Areas not identified are shown by the number of pixels. The entropy formula developed in this study can classify the X-ray test data of children's lungs into three groups: mild pneumonia, severe pneumonia, and normal. The limitation of this study is that it heavily relies on the quality of the input images, particularly those with clear contrast between the lungs and the affected areas. If the images are of poor quality or contain noise, the model's performance may be significantly impacted, despite the existence of techniques for enhancing contrast and noise removal. Although the EVA-GLCM algorithm demonstrated high accuracy (97.5%), this comparison may not be entirely fair if the same datasets were not used or if the datasets in other studies differed in quality or size.

6 REFERENCES

- [1] S. Hooli *et al.*, "In-hospital mortality risk stratification in children aged under 5 years with pneumonia with or without pulse oximetry: A secondary analysis of the Pneumonia research partnership to assess WHO recommendations (PREPARE) dataset," *Int. J. Infect. Dis.*, vol. 129, pp. 240–250, 2023. <https://doi.org/10.1016/j.ijid.2023.02.005>
- [2] K. Nakashima *et al.*, "Effectiveness of the 23-valent pneumococcal polysaccharide vaccine against community-acquired pneumonia in older individuals after the introduction of childhood 13-valent pneumococcal conjugate vaccine: A multicenter hospital-based case-control study in Japan," *Vaccine*, vol. 40, no. 46, pp. 6589–6598, 2022. <https://doi.org/10.1016/j.vaccine.2022.09.055>
- [3] A. G. Mathioudakis *et al.*, "Clinical trials of pneumonia management assess heterogeneous outcomes and measurement instruments," *J. Clin. Epidemiol.*, vol. 164, pp. 88–95, 2023. <https://doi.org/10.1016/j.jclinepi.2023.10.011>
- [4] T. Miyazaki *et al.*, "Community-acquired pneumonia incidence in adults aged 18 years and older in Goto City, Japan," *CHEST Pulm.*, vol. 1, no. 2, pp. 1–17, 2023. <https://doi.org/10.1016/j.chpulm.2023.100007>
- [5] A. Ito, M. Kawataki, R. Sato, Y. Nakanishi, and T. Ishida, "Three cases of hospitalized Legionella pneumonia patients successfully treated with lascefloxacin," *J. Infect. Chemother.*, vol. 31, no. 1, 2024. <https://doi.org/10.1016/j.jiac.2024.05.011>
- [6] D. Koulenti *et al.*, "Protocol for an international, multicentre, prospective, observational study of nosocomial pneumonia in intensive care units: The PneumoINSPIRE study," *Crit. Care and Resusc.*, vol. 23, no. 1, pp. 59–66, 2021. <https://doi.org/10.51893/2021.1.OA5>
- [7] K. N. Yoon *et al.*, "Extending shelf life and analyzing dosimetric and detection techniques in postharvest tomatoes (*Solanum lycopersicum*) via X-ray irradiation," *LWT*, vol. 201, p. 116230, 2024. <https://doi.org/10.1016/j.lwt.2024.116230>

- [8] Hang Yin *et al.*, “Retinomorph X-ray detection using perovskite with hydrion-conductive organic cations,” *The Innov.*, vol. 5, no. 4, 2021. <https://doi.org/10.1016/j.xinn.2024.100654>
- [9] A. S. Alshabibi, W. M. Alyami, and S. F. Alhujaili, “No spectators in a pandemic: A comparison of radiologists, radiology residents, and CT technicians in interpreting chest CT scans for COVID-19,” *J. Radiat. Res. Appl. Sci.*, vol. 17, no. 3, p. 101007, 2024. <https://doi.org/10.1016/j.jrras.2024.101007>
- [10] S. Constantine, A. Salter, J. Louise, and P. J. Anderson, “The Adelaide Facial Bone Rule: A simple prediction model and clinical guideline for the presence of facial fractures using CT brain scans in victims of minor trauma,” *Injury*, vol. 55, no. 5, pp. 1–6, 2024. <https://doi.org/10.1016/j.injury.2023.111302>
- [11] A. N. Mumuni *et al.*, “Scan with Me (SWiM): A train-the-trainer program to upskill MRI personnel in low- and middle- income countries,” *J. Am. Coll. Radiol. (JACR)*, vol. 21, no. 8, pp. 1222–1234, 2024. <https://doi.org/10.1016/j.jacr.2024.04.026>
- [12] A. Jullienne *et al.*, “Musculoskeletal perturbations of deep space radiation: Assessment using a Gateway MRI,” *Life Sci. Sp. Res.*, vol. 42, pp. 74–83, 2024. <https://doi.org/10.1016/j.lssr.2024.05.004>
- [13] Z. Huang *et al.*, “Spatial metabolomics reveal mechanisms of dexamethasone against pediatric pneumonia,” *J. Pharm. Biomed. Anal.*, vol. 229, no. 115369, 2023. <https://doi.org/10.1016/j.jpba.2023.115369>
- [14] R. E. S. Pierre-Hetz, B. S. Skotnicki, C. R. Aspiotes, B. McAninch, and J. R. Rosen, “Shortening treatment duration for uncomplicated community acquired pneumonia to align with best practice guidelines in a large academic paediatric emergency department,” *Futur. Healthc. J.*, vol. 11, no. 2, p. 100142, 2024. <https://doi.org/10.1016/j.fhj.2024.100142>
- [15] H. Kato, M. Hagihara, N. Asai, H. Mikamo, and T. Iwamoto, “Evaluation of effectiveness, hyperkalaemia, and hepatotoxicity of trimethoprim-sulphamethoxazole prophylaxis for *Pneumocystis jirovecii* pneumonia in paediatric patients: A single-centre retrospective study,” *Int. J. Antimicrob. Agents*, vol. 63, no. 5, p. 107151, 2024. <https://doi.org/10.1016/j.ijantimicag.2024.107151>
- [16] Z. Gao *et al.*, “Retrospective computed tomography assessment of chemotherapy-related pneumonia with severity screening in pediatric acute lymphoblastic leukemia by radiological imaging,” *Heliyon*, vol. 10, no. 1, pp. 1–12, 2024. <https://doi.org/10.1016/j.heliyon.2023.e23444>
- [17] N. Barakat, M. Awad, and B. A. Abu-Nabah, “A machine learning approach on chest X-rays for pediatric pneumonia detection,” *Digit. Heal.*, vol. 9, 2023. <https://doi.org/10.1177/20552076231180008>
- [18] I. A. Ahmed, E. M. Senan, H. S. A. Shatnawi, Z. M. Alkhraisha, and M. M. A. Al-Azzam, “Multi-techniques for analyzing X-ray images for early detection and differentiation of pneumonia and tuberculosis based on hybrid features,” *Diagnostics*, vol. 13, no. 4, p. 814, 2023. <https://doi.org/10.3390/diagnostics13040814>
- [19] S. Agrawal and Y. K. Gupta, “Classification of pneumonia lungs infected X-ray images using statistical based features,” vol. 10, pp. 2493–2502, 2023.
- [20] Y. Bi, C. Jiang, H. Qi, H. Zhou, and L. Sun, “Computed tomography image texture under feature extraction algorithm in the diagnosis of effect of specific nursing intervention on mycoplasma pneumonia in children,” *J. Healthc. Eng.*, vol. 2021, no. 1, pp. 1–10, 2021. <https://doi.org/10.1155/2021/6059060>
- [21] A. Onim, S. Musyoki, and P. Kihato, “Selection of optimal SINR threshold in fractional frequency reuse by comparing Otsu’s and entropy method,” *Heliyon*, vol. 8, no. 11, pp. 1–10, 2022. <https://doi.org/10.1016/j.heliyon.2022.e11736>
- [22] K. Nandhini and R. Porkodi, “A new fusion of mutual information and Otsu multilevel thresholding technique for hyperspectral band selection,” *Egypt. Informatics J.*, vol. 22, no. 2, pp. 133–143, 2021. <https://doi.org/10.1016/j.eij.2020.06.002>

- [23] R. V. Manjunath and N. Yashaswini Gowda, "Automated segmentation of liver tumors from computed tomographic scans," *J. Liver Transplant.*, vol. 15, p. 100232, 2024. <https://doi.org/10.1016/j.liver.2024.100232>
- [24] M. K. Wyburd, N. K. Dinsdale, M. Jenkinson, and I. L. Namburete, "Anatomically plausible segmentations: Explicitly preserving topology through prior deformations," *Med. Image Anal.*, vol. 97, p. 103222, 2024. <https://doi.org/10.1016/j.media.2024.103222>
- [25] S. Saifullah and R. Drezewski, "Non-destructive egg fertility detection in incubation using SVM classifier based on GLCM parameters," *Procedia Comput. Sci.*, vol. 207, pp. 3248–3257, 2022. <https://doi.org/10.1016/j.procs.2022.09.383>
- [26] K. V. Ranjitha and T. P. Pushphavathi, "Analysis on improved Gaussian-Wiener filtering technique and GLCM based feature extraction for breast cancer diagnosis GLCM based feature extraction for breast cancer diagnosis," *Procedia Comput. Sci.*, vol. 235, pp. 2857–2866, 2024. <https://doi.org/10.1016/j.procs.2024.04.270>
- [27] S. Bakheet and A. Al-Hamadi, "Automatic detection of COVID-19 using pruned GLCM-based texture features and LDCRF classification," *Comput. Biol. Med.*, vol. 137, no. 104781, 2021. <https://doi.org/10.1016/j.compbiomed.2021.104781>
- [28] Priyanka and D. Kumar, "Feature extraction and selection of kidney ultrasound images using GLCM and PCA," *Procedia Comput. Sci.*, vol. 167, pp. 1722–1731, 2020. <https://doi.org/10.1016/j.procs.2020.03.382>
- [29] C. Nyasulu *et al.*, "A comparative study of machine learning-based classification of tomato fungal diseases: Application of GLCM texture features," *Heliyon*, vol. 9, no. 11, pp. 1–12, 2023. <https://doi.org/10.1016/j.heliyon.2023.e21697>
- [30] G. K. Afolabi-Yusuf, Y. O. Olatunde, K. Y. Obiwusi, M. O. Yusuf, and O. C. Abikoye, "Performance analysis of selected classification algorithms on android malware detection," *International Journal of Software Engineering and Computer Systems (IJSECS)*, vol. 9, no. 2, pp. 140–149, 2024. <https://doi.org/10.15282/ijsecs.9.2.2023.7.0118>
- [31] Muhammad Umar Diggins, S. Usman, S. K. Sanchi, M. Idris, and S. A. Zagga, "Securing IoT healthcare applications and blockchain: Addressing security attacks," *International Journal of Software Engineering and Computer Systems (IJSECS)*, vol. 9, no. 2, pp. 119 – 128, 2023. <https://doi.org/10.15282/ijsecs.9.2.2023.5.0116>
- [32] N. Muthu, F. Abdul Aziz, L. N. Abdullah, M. Mokhtar, M. K. Omar, and M. A. M. Nazar, "The mobile augmented reality application for improving learning of electronic component module in TVET," *International Journal of Software Engineering and Computer Systems (IJSECS)*, vol. 9, no. 2, pp. 82–92, 2023. <https://doi.org/10.15282/ijsecs.9.2.2023.2.0113>

7 AUTHORS

Eva Rianti is a Lecturer at the Universitas Putra Indonesia YPTK Padang, serving as a lecturer in the information system program within the Faculty of Computer Science. Her academic journey includes completing her undergraduate education (S1) in the information system study program at the Universitas Putra Indonesia YPTK Padang, followed by Master's (S2) in UPI YPTK Padang and right now continued study at Doctoral (S3) degrees in the information technology study program at UPI YPTK Padang. Presently, she is offering a diverse array of courses in the information technology study program, such as image processing and artificial intelligence, for communication, she can be reached via email at evarianti@upiyptk.ac.id.

Iskandar Fitri is a Professor at the Universitas Putra Indonesia YPTK Padang, serving as a lecturer in the information technology doctorate program within the Faculty of Computer Science. His academic journey includes completing his undergraduate education (S1) in the electronics engineering study program at Universitas

Nasional, followed by Master's (S2) and Doctoral (S3) degrees in the electronics engineering study program at Universitas Indonesia. Presently, he is recognized as a professor specializing in the microwave field at UPI YPTK Padang. He offers a diverse array of courses in the information technology study program, such as microwaves, research methodology, and artificial intelligence, for communication, he can be reached via email at if@upiypk.ac.id.

Sumijan is a Lecturer and an Associate Professor in the Information Technology (S3) Study Program within the Faculty of Computer Science at the Universitas Putra Indonesia YPTK Padang, Indonesia. He earned his Bachelor's Degree from Universitas Putra Indonesia YPTK Padang in the Information System program under the Faculty of Computer Science. Subsequently, he pursued a Master's Degree at University Technology Malaysia (UTM). And he pursued a doctoral degree from Gunadarma University. Currently, Sumijan is Vice Rector I from Universitas Putra Indonesia YPTK Padang. Sumijan unique identifier, Scopus ID, is 57194787076. His research endeavors traverse diverse domains, with particular expertise in image processing, information system, web design etc. Sumijan welcomes communication and collaboration, and he can be reached via email at sumijan@upiypk.ac.id.

Finny Fitry Yani is a consultant of pediatric respirology since 2011. She works as academic and clinical staff at Department of Child Health, Faculty of Medicine Universitas Andalas & Dr. M. Djamil Hospital, Padang, Indonesia, and member of Indonesian Pediatrics College since 2004. She had several publication about childhood tuberculosis, pneumonia and asthma. She finished the Doctoral study at 2017, with doctoral research about vitamin D to prevent TB infection among children contact TB. Since 2010, she is active as Pediatric TB working groups National tuberculosis Program Health Ministry and 2017 as Executive Secretary in Indonesian TB research network. Since 2020 she is a member of Expert Committee National Tuberculosis Program of Health Ministry. For communication, she can be reached via email at finny_fy@yahoo.com.